substance: chalcogenides of Fe, Ru, Os
property: crystal structure, chemical bond, general characterization

In the Fe – S system, the mixed-valence compounds such as Fe_7S_8 and Fe_3S_4 are metallic. FeS tends to be iron-poor and crystallizes in three polymorphs: hexagonal troilite (B8 with a = 5.962 Å, c = 11.75 Å) [70E], tetragonal mackinawite (with a = 3.68 Å, c = 5.04 Å) [65B] and a cubic phase (B3 with a = 5.42 Å) [78W]. Troilite contains high-spin Fe^{2+} ions [62S], and the five parallel-spin electrons are localized with energies below the Fermi energy, which lies in the band of minority-spin 3d orbitals of $t_{2g} = a_1 + e_\pi$ parentage. There is one minority-spin 3d electron per iron atom, and at high temperatures these minority-spin electrons are itinerant, making troilite metallic above the magnetic-ordering temperature T_N = 600 K [82G]. Below T_N a $d\sigma/dT > 0$ is characteristic of a semiconductor, but a sharp drop in conductivity only occurs below a first-order transition at T_α. In the low-temperature 2C-phase below T_α, the iron atoms form triangular clusters within the basal planes of the B8 (1C) phase to give superlattice cell parameters $a = 3^{1/2}\ a_0$, $c = 2c_0$. In this phase, the minority-spin electrons are trapped in the triangular clusters by splitting of the e_π minority-spin band. A change of the spin orientation from perpendicular to parallel to the c axis on lowering the temperature through $T_s > T_\alpha$ see Fig. 1a, does not significantly change the conductivity. The structure changes smoothly from B8 to B31 on cooling through T_s [78K, 82T]. The temperature T_α decreases and its associated hysteresis increases with increasing x in $Fe_{1-x}S$. The magnetic susceptibility data reveals the spin flip transition at T_s as well as a sharp increase in magnetic anisotropy at T_α and the conventional maximum at T_N.

In both the tetragonal and cubic forms of FeS, the Fe(II) ions occupy tetrahedral sites [65B]. Tetragonal FeS is reported to be a semiconductor [65B]. Cubic FeS becomes antiferromagnetic and orthorhombic below T_N = 238 K [78W].

FeS_2, which contains diamagnetic, low-spin Fe(II) ions, has two polymorphs: pyrite and marcasite [55B, 70B1, 70B2]. Of these, pyrite is the more easily synthesized; only natural marcasite crystals are available. Just the opposite situation occurs for $FeSe_2$ and $FeTe_2$. In both structures, the anions form dimers in which the σ^*-antibonding dimeric orbitals have energies above the bottom of the conduction band. The cubic component of the octahedral-site crystal field splits the iron 3d orbitals into filled bands of t_{2g} parentage and empty bands of e_g parentage. In FeS_2, $FeSe_2$ and $FeTe_2$, the conduction band of both marcasite and pyrite phases is associated with the empty 3d orbitals of eg parentage at the low-spin Fe(II) [82G].

The Fe – Se phase diagram near FeSe indicates that FeSe disproportionates into an iron-rich $Fe_{1.04}Se$ α-phase with LiOH structure that is metallic, and an iron-poor β-phase with cation vacancies ordered onto alternate (001) planes of the B8 structure [66S]. Vacancy ordering within these planes occurs at specific compositions: Fe_7Se_8 and Fe_3Se_4. In the range $0.12 \le x \le 0.125$, the $Fe_{1-x}Se$ phase orders ferrimagnetically below $T_C = (445 + 160x)$ K, ferromagnetic (001) planes of high-spin iron coupling antiparallel [56H, 66S]. Although most authors report that these phases are metallic, Fig. 2 shows data indicative of a metal-semiconductor transition at $T \approx 350$ K < T_N typical of a degenerate semiconductor. Moreover, a phase corresponding to Fe_2Se_3 is included.

Of the iron tellurides, only $FeTe_2$ appears to be semiconducting. However, pressed powders of $Fe_{1-x}Te$ were reported to exhibit semiconducting behaviour at higher temperatures ($T > T_C$) with a change from n to p-type conduction at Fe_2Te_3 [64A].

The RuX_2 and OsX_2 phases are analogous to the FeX_2 pyrite phases; the Ru(II) and Os(II) have low-spin d^6 configurations [63H].

References:

55B Benoit, R.: J. Chim. Phys. 52 (1955) 119.
56H Hirone, T., Chiba, S.: J. Phys. Soc. Jpn. 11 (1956) 666.
62S Sparks, J. T., Mead, W., Komoto, T.: J. Phys. Soc. Jpn. 17, Suppl. B-I (1962) 249.
63H Hulliger, F.: Nature (London) 200 (1963) 1064.
64A Aramu, F., Manca, P.: Nuovo Cimento 34 (1964) 1025.
64K Kullerud, G.: Fortschr. Mineral. 41 (1964) 235.
65B Bertaut, E. F., Burlet, P., Chappert, J.: Solid State Commun. 3 (1965) 335.
66S Serre, J., Druille, R.: Compt. Rend. Ser. B 262 (1966) 639.
70B1 Brostigen, G., Kjekshus, A.: Acta Chem. Scand. 24 (1970) 1925.
70B2 Brostigen, G., Kjekshus, A.: Acta Chem. Scand. 24 (1970) 2993.
70E Evans, H. T.: Science 167 (1970) 621.
71N Nakazawa, H., Morimoto, N.: Mater. Res. Bull. 6 (1971) 345.
73A Akhmedov, N. R., Dzhalilov, N. Z., Abdinov, D. Sh.: Inorg. Mater. 9 (1973) 1271.
76H Horwood, J. L., Townsend, M. G., Webster, A. H.: J. Solid State Chem. 17 (1976) 35.
78K King, H. E., Prewiti, C. T.: Phys. Chem. Minerals 3 (1978) 72.
78W Wintenberger, M., Buevoz, J. L.: Solid State Commun. 27 (1978) 511.
82G Goodenough, J. B.: Ann. Chim. (Paris) 7 (1982) 489.
82T Töpel-Schadt, J., Müller, W. F.: Phys. Chem. Minerals 8 (1982) 175.

Fig. 1.

Fe_xS. (a) T_α and T_s vs. composition (different symbols correspond to different measurements) [76H], (b) phase diagram of the FeS – Fe_7S_8 system (the inserts show two possible phase relations, see original paper) [71N], (c) phase diagram of the Fe – S system [64K].

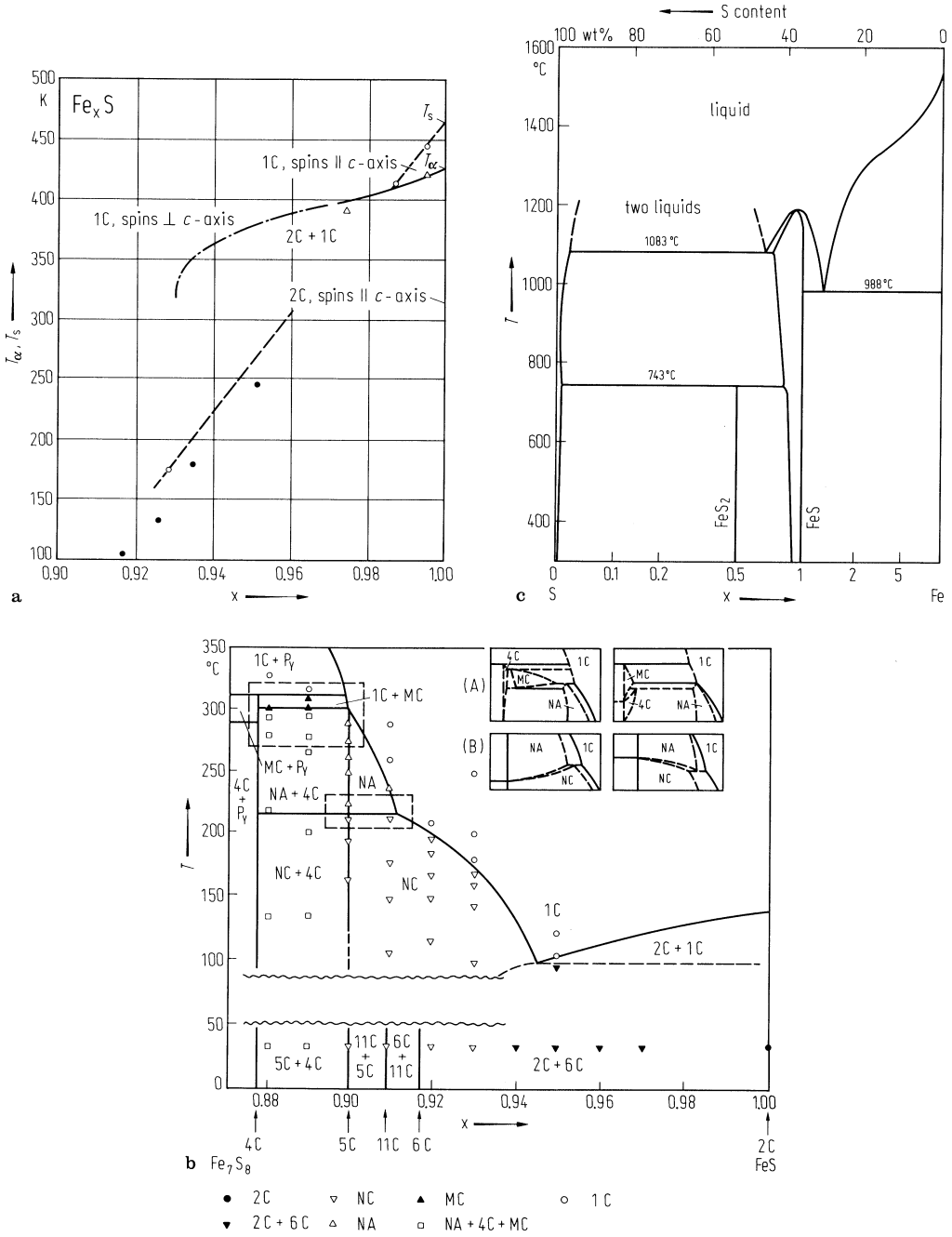

Fig. 2.

Electrical conductivity (a) and thermoelectric power (b) vs. reciprocal temperature for *1*: Fe_7Se_8, *2*: Fe_3Se_4, *3*: Fe_2Se_3, *4*: FeSe [73A]. Polycrystalline samples.